Short Papers

Fingerprint Matching Using an Orientation-Based Minutia Descriptor

Marius Tico, *Member*, *IEEE*, and
Pauli Kuosmanen, *Member*, *IEEE*

Abstract—We introduce a novel fingerprint representation scheme that relies on describing the orientation field of the fingerprint pattern with respect to each minutia detail. This representation allows the derivation of a similarity function between minutiae that is used to identify corresponding features and evaluate the resemblance between two fingerprint impressions. A fingerprint matching algorithm, based on the proposed representation, is developed and tested with a series of experiments conducted on two public domain collections of fingerprint images. The results reveal that our method can achieve good performance on these data collections and that it outperforms other alternative approaches implemented for comparison.

Index Terms—Fingerprints, matching, minutiae, orientation features.

1 Introduction

Fingerprints are graphical ridge patterns present on human fingers, which, due to their uniqueness and permanence, are among the most reliable human characteristics that can be used for people identification [1]. A common hypothesis, is that certain features of the fingerprint ridges, called minutiae, are able to capture the invariant and discriminatory information present in the fingerprint image. The two most prominent types of minutiae, commonly used in automatic fingerprint matching, are ridge ending and ridge bifurcation. A minutia detected in a fingerprint image can be characterized by a list of attributes that includes: 1) the type of minutia (ending or bifurcation), 2) the minutia position with respect to the image frame, and 3) the minutia direction which is defined as the angle that the ridge associated with the minutia makes with the horizontal axis [2]. The internal representation of the fingerprint pattern comprises the attributes of all detected minutiae in a so called minutiae list. A necessary foundation for achieving good matching performance is to establish a realistic model of the variations that may occur between two minutiae lists extracted from different impressions of the same finger [3]. Common assumptions underlying such a model are as follows:

1. the minutiae detection algorithm may deliver spurious minutiae and miss genuine minutiae from both impressions,
2. the finger could have been placed at different positions and orientations onto the acquisition sensor, resulting thereby in global translation and rotation of the minutiae pattern,
3. the finger may exert an unevenly distributed pressure onto the acquisition sensor resulting in local nonlinear deformations due to the elasticity of the skin, and
4. there may be only a small amount of overlap between the two impressions such that several minutiae are not "visible" in both instances.

Several approaches to fingerprint matching have been proposed in the literature. These include methods based on optical correlation [4], [5], transform features [6], [7], [8], graph matching [9], structural matching [10], [11], and point pattern matching [3], [12], [13]. The methods proposed by Germain et al. [14], Hrechack and McHugh [10] as well as Wahab et al. [11] use groups of minutiae in order to define local structural features that embrace geometrical invariant properties. The matching is performed based on the pairs of corresponding structural features that are identified between the two fingerprint impressions. The method proposed by Jiang and Yau [15], relies on a similarity measure defined between local structural features, in order to align the two patterns and calculate a matching score between the two minutiae lists. The methods proposed by Ratha et al. in [12] and Jain et al. in [13] are based on point pattern matching. In these methods, the minutiae in each list are regarded as a pattern of points and the fingerprint matching process is divided in two stages, i.e., registration and minutiae pairing. In [12] the generalized Hough transform (GHT) is used to recover the pose transformation between the two impressions, whereas the registration stage is solved in [13] by aligning the ridge curves associated with two corresponding minutiae. After registration, the corresponding pairs of minutiae are identified by imposing certain geometric constraints with respect to their relative position and direction.

In this paper, we develop a method of fingerprint matching that follows the scheme of a point pattern matching approach including the stages of registration and minutiae pairing. In contrast to previous methods based on point pattern matching [3], [12], [13], our approach relies on a novel representation for the fingerprint minutiae. In addition to usual minutiae attributes, the proposed representation, includes a minutia descriptor that incorporates nonminutiae-based information describing the appearance of the fingerprint pattern in a broad region around the minutia. The proposed minutia descriptor is used not only to efficiently solve the correspondence problem between minutia points detected in two fingerprint impressions but also in order to provide additional nonminutiae information for calculating the degree of similarity between the two impressions. In contrast to the local structural features employed by the matching algorithms proposed in [10], [11], [15], the minutia descriptor proposed here is independent of any other minutia detected in the fingerprint pattern and, hence, it is more robust to the erroneous outcomes of the minutia detection algorithm (i.e., missing and spurious minutiae).

The minutia descriptor proposed in this paper exploits the more general idea of using a rich local characterization for shape representation in order to reduce the complexity of feature correspondence and matching problems. Closely related, in this respect, to our approach is the work of Belongie et al. [16]. Regarding a shape as a discrete set of sample contour points, they propose a representation scheme that comprises a coarse distribution of the shape with respect to each point. Since the contour sample points can be chosen in any number, one can always peek enough such points in order to accurately represent the underlying shape. In contrast, the minutia points of a fingerprint capture only a very limited amount of information from the reach information content present in the fingerprint pattern. Consequently, a representation of the fingerprint pattern with respect to each minutia detail must employ nonminutia information like brightness, ridge orientation, transform features, etc. In this work, we investigate the use of orientation information for minutia representation in the context of the fingerprint pattern. We start by defining in Section 2 the terms of relative orientation and orientation distance that both play a central role in our approach. The proposed minutia descriptor is introduced in Section 3. In Section 4, we present a fingerprint matching scheme that relies on the proposed representation. The experimental results, presented in Section 5 of the paper, assess the performance of our approach on two public domain collections of fingerprint images. Finally, concluding remarks are presented in Section 6.

2 Definitions

In this work, we make a distinction between the terms direction and orientation. The former refers to angles in the range $[0, 2\pi)$, whereas

- *M. Tico is with the Nokia Research Center, PO Box 100, FIN-33721 Tamere, Finland. E-mail: tico@ieee.org.*
- *P. Kuosmanen is with the Institute of Signal Processing, Tampere University of Technology, PO Box 553, FIN-33101 Tampere, Finland. E-mail: pauli.kuosmanen@tut.fi.*

Manuscript received 15 Oct. 2001; revised 18 Apr. 2002; accepted 14 July 2002. Recommended for acceptance by M. Pietikainen.
For information on obtaining reprints of this article, please send e-mail to: tpami@computer.org, and reference IEEECS Log Number 115193.

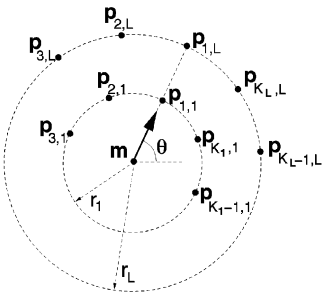

Fig. 1. Sampling points organized in a circular pattern around a minutia detail.

the latter designates angles in the range $[0, \pi)$. For instance, we can say that two vectors of opposite directions θ and $\theta + \pi$, respectively, are both along a line of orientation θ.

Let α and β denote two orientation angles. We define the relative orientation of α with respect to β, denoted by $\lambda(\alpha, \beta)$, as the minimum angle required to rotate a line of orientation β in the counterclockwise sense such that to make it parallel with a line of orientation α.

In order to evaluate the dissimilarity between orientation angles, we employ the metric

$$\Lambda(\alpha, \beta) = (2/\pi) \min\{\lambda(\alpha, \beta), \lambda(\beta, \alpha)\}, \tag{1}$$

called orientation distance, which takes values between 0 and 1 achieving the two extrema for parallel and orthogonal orientations, respectively.

3 The Orientation-Based Minutia Descriptor

According to the taxonomy proposed by Rao in [17], fingerprints can be classified as weakly-order textures exhibiting a dominant ridge orientation at each point. The orientation field provides a rough description of the fingerprint pattern that can be estimated with reasonable accuracy even from noisy input images. We propose to characterize the location of each minutia with respect to the input fingerprint pattern based on a descriptor that comprises information about the orientation field in a broad region around the minutia point. Since the ridge orientation typically exhibits small spatial variations between neighborhood pixels, a large area of the orientation field can be reconstructed from the orientation angles estimated in a relatively small number of sampling points. The sampling points assigned to each minutia can be organized in a circular pattern around the minutia position $\mathbf{m} = [x, y]^T$, as illustrated in Fig. 1.

The circular pattern consists of L concentric circles of radii r_ℓ, $(1 \le \ell \le L)$, each one of them comprising K_ℓ sampling points $\mathbf{p}_{k,\ell}$, $(1 \le k \le K_\ell)$, equally distributed along its circumference. Using the minutia direction (θ) as a reference, the points on each circle can be ordered in a counterclockwise manner starting with the point located along θ with respect to the minutia position. Denoting by $\theta_{k,\ell}$ the local ridge orientation estimated in $\mathbf{p}_{k,\ell}$, we define the minutia descriptor as follows:

$$\mathbf{f} = \left\{ \left\{ \lambda(\theta_{k,\ell}, \theta) \right\}_{k=1}^{K_\ell} \right\}_{\ell=1}^{L}. \tag{2}$$

The minutia descriptor (2) is invariant to rotation and translation and, hence, it may characterize the minutia location with respect to the fingerprint pattern regardless of the position and orientation of the finger onto the acquisition sensor. In addition, a useful property of the proposed descriptor consists of its independence with respect to any other minutia detected in the input image.

3.1 The Selection of the Sampling Points

The selection of the parameters r_ℓ and K_ℓ might be regarded as a sampling problem, where the goal is to build a representation that allows reconstruction of the orientation field over a broad region around each minutia point. We propose to select the sampling points around each minutia such that to preserve a minimum distance of 2τ (pixels) between them, where τ denotes the average fingerprint ridge period. On one hand, this is accomplished by imposing a minimum difference of 2τ between the values of the consecutive radii r_ℓ and $r_{\ell+1}$. On the other hand, the number of points (K_ℓ) on the ℓth circle can be calculated by imposing the prescribed minimum distance between any two adjacent points $\mathbf{p}_{k,\ell}$ and $\mathbf{p}_{k+1,\ell}$. This results in the formula $K_\ell = \lceil \pi r_\ell / \tau \rceil$, where $\lceil x \rceil$ stands for the smallest integer value larger than x. Assuming an average value of 0.463 mm for the ridge period, as reported in [18] and denoting by R the image resolution expressed in dots per inch (dpi), we can rewrite the previous formula as $K_\ell = \lceil 172 \cdot r_\ell / R \rceil$.

3.2 The Similarity Function

Let a and b denote the labels associated with two minutiae whose descriptors (2) are, respectively, $\mathbf{f}(a) = \{\alpha_{k,\ell}\}$ and $\mathbf{f}(b) = \{\beta_{k,\ell}\}$. A similarity function between minutiae is defined as

$$S(a, b) = (1/K) \sum_{\ell=1}^{L} \sum_{k=1}^{K_\ell} s\big(x_{k,\ell}\big), \tag{3}$$

where $K = \sum_{\ell=1}^{L} K_\ell$, $x_{k,\ell} = \Lambda(\alpha_{k,\ell}, \beta_{k,\ell})$, and $s(x)$ denotes a similarity value between angles that are displaced by an orientation distance x.

For any pair of minutiae detected in two different fingerprint images, we can distinguish between two hypothesis: the hypothesis $\mathcal{H}_1$ that the two minutiae are correspondent and the hypothesis $\mathcal{H}_0$ that the two minutiae are not correspondent. Our objective is to design the function s such that to achieve much larger similarity values (3) under $\mathcal{H}_1$ than under $\mathcal{H}_0$.

We assume that the orientation distances $\{x_{k,\ell}\}$, between individual components of minutia descriptors are realizations of independent and identically distributed random variables whose probability density function (p.d.f.) is zero outside $[0, 1]$. An estimate of the conditional p.d.f. $p(x|\mathcal{H}_0)$, that models the orientation distance between features of noncorrespondent minutiae descriptors, was

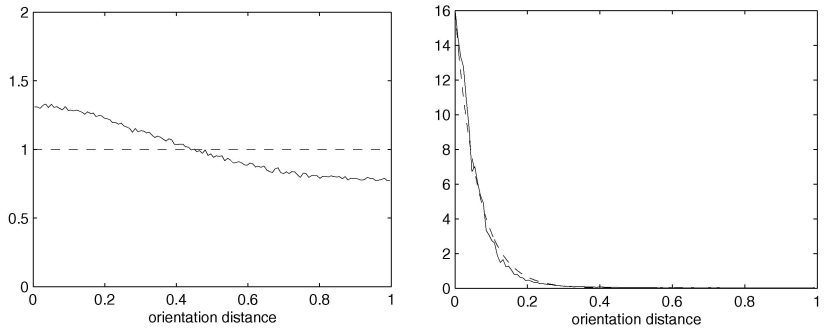

(a) (b)

Fig. 2. The estimated p.d.f. of the orientation distance (continuous line) the theoretical p.d.f. (dashed line) (a) under $\mathcal{H}_0$ and (b) under $\mathcal{H}_1$.

TABLE 1
EERs Estimated on DB2 for Different Values of the Parameters r and K

EER (%)	$K = 10$	$K = 20$	$K = 30$	$K = 40$
$r = 60$	4.03	**3.28**	**3.32**	**3.31**
$r = 90$	4.10	3.75	**3.42**	**3.38**

determined by comparing minutiae that belong to impressions captured from different fingers included in database DB1 [19]. The result shown in Fig. 2a, reveals that the uniform p.d.f. on $[0, 1]$ may constitute an adequate approximation of $p(x|\mathcal{H}_0)$. The requirement to achieve small similarity values (3) between noncorrespondent minutiae can be formally expressed as selecting s such that to reduce the conditional expectation $E\{S^2|\mathcal{H}_0\}$. One can show that

$$E\{S^2|\mathcal{H}_0\} = \frac{1}{K}\int_0^1 s^2(x)dx + \frac{K-1}{K} \times \left(\int_0^1 s(x)dx\right)^2 \leq \int_0^1 s^2(x)dx. \tag{4}$$

Consequently, a sufficient condition to achieve small similarity values (3) under $\mathcal{H}_0$ is to chose a function s that has a small second order moment on $[0, 1]$.

On the other hand, in order to achieve large similarity values between correspondent minutiae we need to chose s such that to maximize the conditional expectation

$$E\{S|\mathcal{H}_1\} = E\{s|\mathcal{H}_1\} = \int_0^1 s(x)p(x|\mathcal{H}_1)dx, \tag{5}$$

where $p(x|\mathcal{H}_1)$ models the distance between orientation features collected from sampling points that belong to correspondent minutiae. Combining the two requirements for s, we can formulate our objective as to design s such that to maximize the functional

$$J(s) = \left(\int_0^1 s(x)p(x|\mathcal{H}_1)dx\right)^2 / \left(\int_0^1 s^2(x)dx\right), \tag{6}$$

which, according to Cauchy-Schwartz inequality, results in

$$s(x) = \kappa p(x|\mathcal{H}_1), \tag{7}$$

where κ is an arbitrary constant.

A model for $p(x|\mathcal{H}_1)$ has been established empirically based on the histogram of observed orientation distances between components of corresponding minutiae descriptors. For this experiment, we selected 40 pairs of fingerprint images from the database DB1 [19], and manually identified corresponding minutiae between the two images in each pair. The result shown in Fig. 2b, reveals that the exponential p.d.f., normalized such that to integrate to 1 on $[0, 1]$, constitutes a reasonable candidate to fit the original histogram. Consequently, an appropriate form for the orientation similarity function (7) is given by

$$s(x) = \exp(-x/\mu), \tag{8}$$

where, for convenience, we chose κ in formula (7) such that $s(0) = 1$, and the mean μ was empirically set at $1/16$ based on the test images used in the experiment.

4 Fingerprint Matching

Using the proposed minutia descriptor, we developed a fingerprint matching algorithm based on point pattern matching. The algorithm receives at the input two minutiae lists captured from two fingerprint impressions and delivers a matching score that expresses the degree of similarity between the two fingerprints. Let $\mathcal{A} = \{a_i\}_{i=1}^N$ and $\mathcal{B} = \{b_j\}_{j=1}^M$ denote the minutiae lists extracted from the input fingerprint impressions. In order to compute the matching score, we need to identify a set of corresponding minutia pairs $\mathcal{C} = \{(i, j)|\ a_i \in \mathcal{A}, b_j \in \mathcal{B}\}$, where each pair (i, j) designates the labels a_i and b_j that are associated with the same physical detail (minutia) detected in both instances.

4.1 Corresponding Minutiae Identification

The value of the similarity degree between minutiae constitutes an important clue for identifying corresponding pairs. Two minutiae a_i and b_j are likely to be correspondent if their similarity value $S(a_i, b_j)$ is large. However, we may encounter difficulties in distinguishing the correct corresponding pair when, for instance, a_i exhibits a large similarity degree also with respect to another minutiae $b_{j'} \in \mathcal{B}\backslash\{b_j\}$. Such a situation may occur when the minutiae b_j and $b_{j'}$ are close one to each other and, hence, their descriptors may be very similar. In order to identify the most distinguishable pairs of corresponding minutiae, we define the possibility that two minutiae a_i and b_j are correspondent based on the following two requirements: 1) the similarity value $S(a_i, b_j)$ is large and 2) both a_i and b_j exhibit small similarities with respect to other minutia from $\mathcal{B}\backslash\{b_j\}$ and $\mathcal{A}\backslash\{a_i\}$, respectively. Formally, the possibility value is expressed by the following formula

$$\mathrm{P}(a_i, b_j) = S(a_i, b_j)^2 / \left(\sum_{i'=1}^{N} S(a_{i'}, b_j) + \sum_{j'=1}^{M} S(a_i, b_{j'}) - S(a_i, b_j)\right), \tag{9}$$

and it approaches a maximum value of $S(a_i, b_j)$ if both a_i and b_j are highly distinct in comparison with other minutiae from $\mathcal{B}\backslash\{b_j\}$ and $\mathcal{A}\backslash\{a_i\}$, respectively.

4.1.1 Registration

The registration stage is meant to recover the geometric transformation between the two fingerprint impressions in order to bring the minutiae from $\mathcal{A}$ in the spatial proximity of their corresponding counterparts from $\mathcal{B}$. In our work, the parameters of the geometric transformation, i.e., translation vector ($\mathbf{t} = [t_x,\ t_y]^T$) and rotation angle ($\varphi$), are calculated such that to overlap the minutiae pair (a_p, b_q) that exhibits the largest possibility value (9). The underlying assumption, justified by experimental observations, is that a_p and b_q are corresponding minutiae and, hence, we have

$$\varphi = \theta(b_q) - \theta(a_p),\ \text{and}\ \mathbf{t} = \mathbf{m}(b_q) - \mathbf{R}_\varphi \mathbf{m}(a_p), \tag{10}$$

where $\mathbf{R}_\varphi$ denotes the 2×2 operator of counterclockwise rotation with φ and the position and direction of a minutia a are denoted by $\mathbf{m}(a) = [x(a),\ y(a)]^T$ and $\theta(a)$, respectively. Applying the estimated geometric transformation onto the minutiae from $\mathcal{A}$ we obtain the list $\mathcal{A}'$ comprising the registered minutiae.

TABLE 2
EERs and Matching Times Estimated on DB1 and DB2 for Different Configurations of Sampling Points Around Each Minutia

Sampling point configuration: $(r_1, K_1), (r_2, K_2), \ldots, (r_L, K_L)$	DB1		DB2	
	EER (%)	Matching time (msec)	EER (%)	Matching time (msec)
$(42, 14), (60, 20), (78, 26)$	5.3	10	2.6	15
$(42, 14), (60, 20), (78, 26), (96, 32)$	5.2	15	2.3	21
$(27, 10), (45, 16), (63, 22), (81, 28)$	4.9	14	2.3	19

TABLE 3
EERs Estimated on DB1 and DB2 when Different Forms of the Orientation Similarity Function Are Used

	$s(x)$	EER (%)	
		DB1	DB2
1	$\exp(-16x)$	4.9	2.3
2	$u(x) - u(x - 0.1)$	5.2	2.6
3	$1 - x$	10.9	6.8

The function u in the second row stands for the unit step function.

4.1.2 Minutia Pairing

It is unrealistic to expect that the minutiae from $\mathcal{A}'$ will overlap exactly over their corresponding counterparts from $\mathcal{B}$. Because of various factors that include the presence of local nonlinear deformations and the errors induced by the minutiae extraction algorithm, the corresponding minutiae may be displaced one with respect to another. Consequently, one must allow a certain tolerance between the positions and directions of corresponding minutiae by employing an elastic matching algorithm as proposed in [12], [13], and [15].

In our approach, the corresponding minutiae pairs are collected among the pairs with largest possibility values (9), which, also satisfy the following geometric constraints after registration: 1) the Euclidean distance between the two minutiae does not exceed a certain value Δd and 2) the angular difference between their directions is less than a certain tolerance $\Delta\theta$. Both parameters Δd and $\Delta\theta$ are selected empirically being dependent on the image resolution. Their values, however, are not critical for our matching algorithm since the selection of corresponding pairs is mainly guided by the possibility values computed between minutiae of the two lists.

Let $\mathbf{P}$ denote a $N \times M$ matrix that stores the possibility values (9) of all minutia pairs that satisfy the geometric constraints. Thus, $\mathbf{P}_{i,j} = \mathrm{P}(a_i, b_j)$ if the relative position and direction of a'_i and b_j are within the acceptable tolerances and $\mathbf{P}_{i,j} = 0$ otherwise.

The set $\mathcal{C}$ of corresponding minutiae pairs, is constructed using a Greedy algorithm. The first item inserted in $\mathcal{C}$ is the pair (p, q) that corresponds to the minutiae a_p and b_q whose possibility value (9) is maximum. The remaining pairs of corresponding minutiae are successively identified in the decrease order of their possibility values stored in $\mathbf{P}$. At each step, the algorithm includes in $\mathcal{C}$ the pair (i, j) that corresponds to the largest nonzero element of $\mathbf{P}$, following then to reset all those entries of $\mathbf{P}$ that are located on the same row (i) or column (j). The reset operation is meant to guarantee the unique interpretation constraint, which states that a minutia from one list cannot be paired with more than one minutiae from the another list. The algorithm stops when there is no other nonzero element in $\mathbf{P}$.

4.2 Matching Score Computation

As we mentioned in the preamble of this paper, two fingerprint images may share only a small common region such that several minutiae are not "visible" in both instances. Consequently, in order to evaluate the similarity between two fingerprint impressions, we should consider only those minutiae that fall inside the region of interest common to both fingerprints. These minutiae are roughly identified based on the two bounding rectangles defined by the minutiae from $\mathcal{A}'$ and $\mathcal{B}$. Let A_B and B_A denote the number of minutiae from $\mathcal{A}'$ and $\mathcal{B}$, respectively, that are located inside the intersection of the two bounding rectangles. If both A_B and B_A exceed a certain threshold then the matching score can be calculated according to the following formula

$$\frac{1}{A_B B_A}\left(\sum_{(i,j)\in\mathcal{C}} S(a_i, b_j)\right)^2. \tag{11}$$

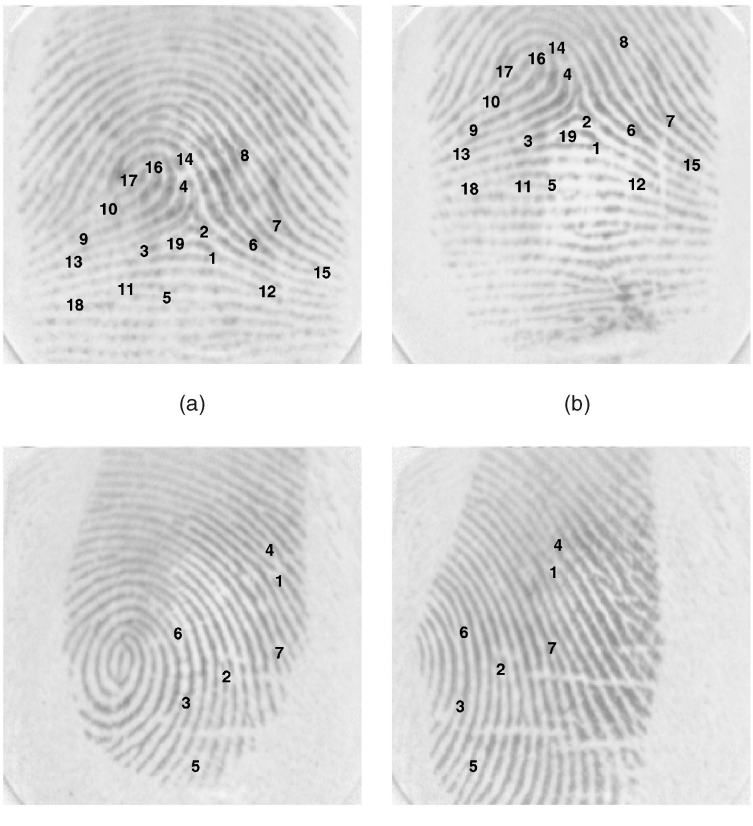

Fig. 3. Corresponding minutiae identified by our algorithm between impressions captured from the same finger, (a) and (b) and (c) and (d), respectively.

TABLE 4
The Number of Incorrect Correspondences (b), over the Total Number of Correspondences (c), Identified by Our Algorithm between Two Impressions of the Fingerprint (a), from DB1

a	1	2	3	4	5	6	7	8	9	10
b / c	0/17	1/25	0/13	0/7	0/20	1/26	1/12	3/24	3/12	0/12
	11	12	13	14	15	16	17	18	19	20
	1/15	1/19	1/9	2/9	2/14	1/24	4/26	2/20	3/26	0/17
	81	82	83	84	85	86	87	88	89	90
	1/17	0/29	2/20	1/21	2/25	1/10	3/20	2/20	1/19	0/18
	91	92	93	94	95	96	97	98	99	100
	4/16	0/10	1/10	3/14	3/19	4/31	0/14	4/4	4/28	3/10

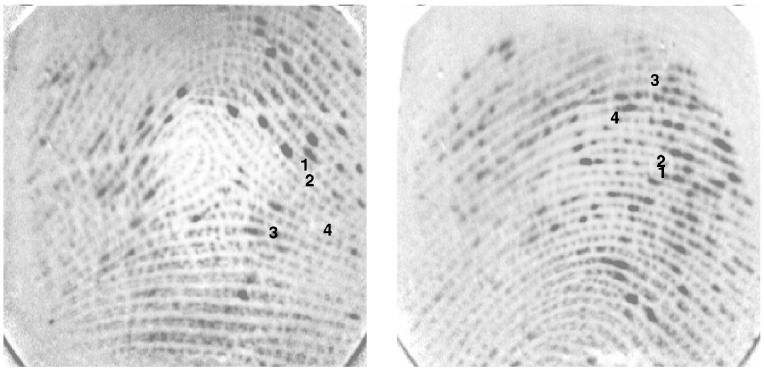

(a) (b)

Fig. 4. Example when the algorithm fails to identify the correct correspondences between two impressions (a) and (b) captured from the same finger.

5 Experimental Results

The experiments reported in this paper have been conducted on two public domain collections of fingerprint images proposed in [19]. Each one of the two data collections, labeled DB1 and DB2, respectively, comprises 800 fingerprint images captured at a resolution of 500 dpi, from 100 fingers (eight impressions per finger). All matching performance indicators shown in this section have been estimated using the experimental protocol proposed in [19].

Although our work focuses only on the fingerprint matching problem it is worthwhile to briefly summarize the procedure employed to extract the fingerprint features used by the following matching experiments. The procedure commences with an image enhancement stage that improves the definition of ridges against valleys by applying the Fourier domain processing described in the work [20] by Candela et al. Next, the fingerprint ridges as well as the region of interest where the fingerprint pattern is located in the input image, are identified based on the second directional derivative of the digital image using the ridge segmentation approach presented in [21]. The binary image delivered by the segmentation algorithm is submitted to a thinning operation following then to detect the minutia details into the thinned representation of the ridge pattern, as described in the work [22]. The orientation angles in different points of the fingerprint pattern are estimated from the enhanced fingerprint image using the approach proposed by Rao in [17].

A first set of experiments have been conducted in order to evaluate the matching performance for different configurations of sampling points used to construct the minutia descriptor. In accordance to the guidelines presented in Section 3.1, for an image resolution of 500 dpi, we can chose $K_\ell \approx \lceil r_\ell/3 \rceil$, $(1 \leq \ell \leq L)$ and a difference of about 18 pixels between consecutive radii. Selecting different numbers (K) of sampling points along a single circle of radius (r) we obtain the results shown in Table 1. These results, expressed in terms of Equal Error Rate (EER), confirm our expectation that the matching performance may not exhibit important variations or improvements when the number of points (K) exceed the maximum prescribed value, which in this case is $r/3$.

The matching performance achieved on DB1 and DB2 for three different configurations of sampling points distributed along more than one circle are shown in Table 2. The table shows also the average execution times for a matching on a Pentium IV, 1.5 GHz. Other matching results estimated on the same data collections can be found in [19], where a number of 11 fingerprint verification algorithms created by different academic groups and companies have been tested. In comparison, the matching performance presented in Table 2 could be placed among the best three results reported in [19].

Table 3 presents the matching performance achieved by using different forms of the orientation similarity function $s(x)$, where x stands for the orientation distance. The first form is the one proposed in (8), which has been also employed in all other matching experiments presented in this section. According to the second form two orientation angles are equivalent iff the orientation distance between them is smaller than a threshold (i.e., 0.1). The third form is a linear function with respect to the orientation distance.

A set of experiments were conducted in order to evaluate the ability of the proposed algorithm to correctly identify corresponding minutiae between fingerprint impressions captured from the same finger. For this purpose, we used the first and the fourth impressions of 40 fingerprints whose labels are $1, \ldots, 20$ and $81, \ldots, 100$ in DB1. The evaluation was carried out by visually inspecting the minutiae correspondences identified by our algorithm between the two impressions of each fingerprint, as exemplified in Fig. 3. The results, shown in Table 4, revealed that, in average, 88.7 percent of corresponding minutiae pairs identified by our algorithm were correct. We noted that the incorrect correspondences are caused by factors like: errors in minutia detection, unreliable orientation estimation in low quality images and small amount of overlap between the two impressions. Such an extreme case, when the algorithm fails, is shown in Fig. 4, for the fingerprint 98.

Next, we conducted a set of experiments meant to evaluate our registration approach described in Section 4.1.1 and, on the other hand, the approaches of minutiae pairing (Section 4.1.2) and matching score computation (Section 4.2) presented in this paper. The generalized Hough transform (GHT) for point pattern matching [12], [23] was implemented as an alternative to our

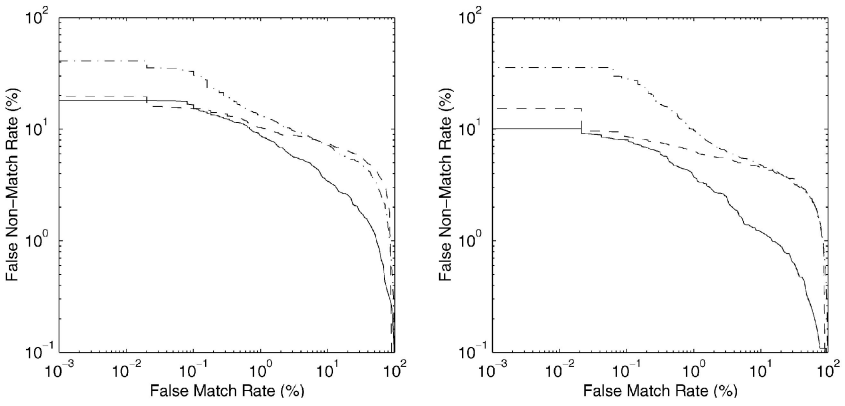

Fig. 5. ROC-curves on (a) DB1 and (b) DB2 obtained with our matching algorithm (solid line), the algorithm A (dashed line), and the algorithm B (dash-dot line).

registration approach. A critical parameter for the GHT approach is the dimension of each bin in the discretized parameter space. After several experiments on both databases, we determined that a very good choice for the bin dimensions is $\pi/32$ along the rotational axis and six pixels along each one of the translational axes. Matching experiments have been performed on both data collections using our algorithm as well as: algorithm A the GHT method for registration in combination with our approaches of minutia pairing and matching score computation and algorithm B the fingerprint matching algorithm proposed in [12] that relies on GHT method in order to register the two minutiae patterns and calculates the matching score based on the number of corresponding minutiae pairs. The Receiver Operating Characteristic (ROC) curves obtained by the three algorithms are shown in Fig. 5.

We note that our algorithm outperforms the algorithm A. The only difference between the two algorithms consists of the method used for minutia registration. Consequently, these results reveal that our registration approach (Section 4.1.1) is able to recover the pose transformation between the two fingerprint impressions more accurately than the GHT method.

Since both algorithms A and B use the same registration method, the discrepancies between their performance are due only to the methods used by each one of them for minutia pairing and matching score computation. The results shown in Fig. 5 are in the favor of algorithm A that uses our approaches described in Section 4.1.2 and Section 4.2. These results reveal that the fingerprint matching algorithm benefits from using the proposed similarity measure between minutia details, being able to decide more accurately whether the two input fingerprint impressions have been captured from the same finger or not.

6 Conclusions

In this paper, we introduced a representation scheme for fingerprint patterns that allows integration of nonminutia features along with the minutia details of the fingerprint. The basic idea consists of describing the appearance of the fingerprint pattern with respect to each landmark point (minutia), in an attempt to capture more characteristic features from the reach information content present in the fingerprint. Our work investigates the integration of ridge orientation information into the fingerprint representation. This representation: provides additional nonminutiae information for calculating a more reliable degree of similarity between fingerprint impressions; allows the design of a low complexity algorithm for solving the feature correspondence problem; and reduces the interdependencies between minutia details, which can be missed or erroneously detected by a minutiae extraction algorithm. A fingerprint matching algorithm that relies on the proposed representation has been developed and tested on two public domain collections of fingerprint images.

References

[1] *BIOMETRICS Personal Identification in Networked Society.* A.K. Jain, R. Bolle, S. Pankanti, eds., Kulwer Academic, 1999.
[2] H.C. Lee and R.E. Gaensslen, *Advances in Fingerprint Technology.* CRC Press, 1991.
[3] A.K. Jain, L. Hong, S. Pankanti, and R. Bolle, "An Identity-Authentication System Using Fingerprints," *Proc. IEEE,* vol. 85, no. 9, pp. 1365-1388, 1997.
[4] C. Wilson, C. Watson, and E. Paek, "Effect of Resolution and Image Quality on Combined Optical and Neural Network Fingerprint Matching," *Pattern Recognition,* vol. 33, no. 2, pp. 317-331, 2000.
[5] F. Gamble, L. Frye, and D. Grieser, "Real-Time Fingerprint Verification System," *Applied Optics,* vol. 31, no. 5, pp. 652-655, 1992.
[6] A.K. Jain, S. Prabhakar, L. Hong, and S. Pankanti, "Filterbank-Based Fingerprint Matching," *IEEE Trans. Image Processing,* vol. 9, no. 5, pp. 846-859, 2000.
[7] C.J. Lee and S.D. Wang, "Fingerprint Feature Extraction Using Gabor Filters," *Electronics Letters,* vol. 35, no. 4, pp. 288-290, 1999.
[8] M. Tico, P. Kuosmanen, and J. Saarinen, "Wavelet Domain Features for Fingerprint Recognition," *Electronics Letters,* vol. 37, no. 1, pp. 21-22, 2001.
[9] D.K. Isenor and S.G. Zaky, "Fingerprint Identification Using Graph Matching," *Pattern Recognition,* vol. 19, no. 2, pp. 113-122, 1986.
[10] A.K. Hrechak and J.A. McHugh, "Automatic Fingerprint Recognition Using Structural Matching," *Pattern Recognition,* vol. 23, no. 8, pp. 893-904, 1990.
[11] A. Wahab, S.H. Chin, and E.C. Tan, "Novel Approach to Automated Fingerprint Recognition," *IEE Proc. Visual Image Signal Processing,* vol. 145, no. 3, pp. 160-166, 1998.
[12] N.K. Ratha, K. Karu, S. Chen, and A.K. Jain, "A Real-Time Matching System for Large Fingerprint Databases," *IEEE Trans. Pattern Analysis and Machine Intelligence,* vol. 18, no. 8, pp. 799-813, Aug. 1996.
[13] A.K. Jain, L. Hong, and R. Bolle, "On-Line Fingerprint Verification," *IEEE Trans. Pattern Analysis and Machine Intelligence,* vol. 19, no. 4, pp. 302-313, Apr. 1997.
[14] R.S. Germain, A. Califano, and S. Colville, "Fingerprint Matching Using Transformation Parameter Clustering," *IEEE Computational Science and Eng.,* vol. 4, no. 4, pp. 42-49, 1997.
[15] X. Jiang and W.-Y. Yau, "Fingerprint Minutiae Matching Based on the Local and Global Structures," *Proc. 15th Int'l Conf. Pattern Recognition,* vol. 2, pp. 1038-1041, 2000.
[16] S. Belongie, J. Malik, and J. Puzicha, "Matching Shapes," *Proc. Eighth IEEE Int'l Conf. Computer Vision (ICCV),* vol. 1, pp. 454-461, 2001.
[17] A.R. Rao, *A Taxonomy for Texture Description and Identification.* Springer-Verlag, 1990.
[18] D.A. Stoney, "Distribution of Epidermal Ridge Minutiae," *Am. J. Physical Anthropology,* vol. 77, pp. 367-376, 1988.
[19] D. Maio, D. Maltoni, R. Cappelli, J.L. Wayman, and A.K. Jain, "FVC2000: Fingerprint Verification Competition," *IEEE Trans. Pattern Analysis and Machine Intelligence,* vol. 24, no. 3, pp. 402-412, Mar. 2002.
[20] G.T. Candela, P.J. Grother, C.I. Watson, R.A. Wilkinson, and C.L. Wilson, "PCASYS—A Pattern-Level Classification Automation System for Fingerprints," Technical Report NISTIR 5647, 1995.
[21] M. Tico, "On Design and Implementation of Fingerprint-Based Biometric Systems," PhD thesis, Tampere Univ. of Technology, Tampere, Finland, 2001.
[22] M. Tico and P. Kuosmanen, "An Algorithm for Fingerprint Image Postprocessing," *Proc. 34th Asilomar Conf. Signals, Systems and Computers,* vol. 2, pp. 1735-1739, 2000.
[23] D.H. Ballard, "Generalized Hough Transform to Detect Arbitrary Patterns," *IEEE Trans. Pattern Analysis and Machine Intelligence,* vol. 3, no. 2, pp. 111-122, 1981.